AGU PUBLICATIONS

Geophysical Research Letters

RESEARCH LETTER
10.1002/2015GL066281

Key Point:
- Pacific climate variability arises from the interaction of ENSO and Pacific Meridional Modes

Correspondence to:
E. Di Lorenzo,
edl@gatech.edu

Citation:
Di Lorenzo, E., G. Liguori, N. Schneider, J. C. Furtado, B. T. Anderson, and M. A. Alexander (2015), ENSO and meridional modes: A null hypothesis for Pacific climate variability, *Geophys. Res. Lett.*, *42*, doi:10.1002/2015GL066281.

Received 25 SEP 2015
Accepted 9 OCT 2015
Accepted article online 12 OCT 2015

©2015. American Geophysical Union. All Rights Reserved.

ENSO and meridional modes: A null hypothesis for Pacific climate variability

E. Di Lorenzo[1], G. Liguori[1], N. Schneider[2], J. C. Furtado[3], B. T. Anderson[4], and M. A. Alexander[5]

[1]School of Earth and Atmospheric Sciences, Georgia Institute of Technology, Atlanta, Georgia, USA, [2]International Pacific Research Center, University of Hawai'i at Mānoa, Honolulu, Hawaii, USA, [3]School of Meteorology, University of Oklahoma, Norman, Oklahoma, USA, [4]Department of Earth and Environment, Boston University, Boston, Massachusetts, USA, [5]NOAA/Earth System Research Laboratory, Boulder, Colorado, USA

Abstract Pacific low-frequency variability (timescale > 8 years) exhibits a well-known El Niño-like pattern of basin-scale sea surface temperature, which is found in all the major modes of Pacific decadal climate. Using a set of climate model experiments and observations, we decompose the mechanisms contributing to the growth, peak, and decay of the Pacific low-frequency spatial variance. We find that the El Niño-like interdecadal pattern is established through the combined actions of Pacific meridional modes (MM) and the El Niño–Southern Oscillation (ENSO). Specifically, in the growth phase of the pattern, subtropical stochastic excitation of the MM energizes the tropical low-frequency variance acting as a red noise process. Once in the tropics, this low-frequency variance is amplified by ocean-atmospheric feedbacks as the pattern reaches its peak phase. At the same time, atmospheric teleconnections distribute the variance from the tropics to the extratropics, where the pattern ultimately decays. In this stochastic red noise model of Pacific climate, the timescale of the extra-tropical/tropical interactions (1–2 years) permits the stochastic excitation of the ENSO-like pattern of decadal and interdecadal variance.

1. Introduction

The observed decadal climate of the Pacific has been characterized in terms of statistical patterns of low-frequency oceanic variability, like the Interdecadal Pacific Oscillation [*Trenberth and Hurrell*, 1994; *Power et al*., 1999; *Deser et al*., 2004], the Pacific Decadal Oscillation [*Mantua et al*., 1997], and more recently the North Pacific Gyre Oscillation [*Di Lorenzo et al*., 2008]. Although these patterns track large-scale dynamics of the coupled ocean-atmosphere system and are useful for assessing the state of Pacific climate, the dynamics underlying the origin of the decadal and interdecadal Pacific variance are still debated. In the low-frequency limit (timescales > 8 years), these modes are all characterized by a spatially broad ENSO-like pattern [*Zhang et al*., 1997] (Figures 1a–1d), which is derived by computing the first empirical orthogonal function (EOF) of the 8 year low-pass sea surface temperature anomalies (SSTa) over the Pacific Ocean basin (45°S–65°N) (Figure 1a). The emergence of this ENSO-like pattern, and its spatial symmetry from the equator, suggests that an important fraction of this low-frequency variance originates from tropical Pacific dynamics linked to the ENSO system.

The influence of ENSO on the modes of Pacific decadal variability is well documented by previous studies showing how atmospheric and ocean teleconnections forced by ENSO, and its different eastern and central Pacific expressions, imprint a signal in the extratropics on the Pacific Decadal Oscillation (PDO) and North Pacific Gyre Oscillation (NPGO) [*Alexander et al*., 2002; *Vimont*, 2005; *Di Lorenzo et al*., 2010; *Furtado et al*., 2012]. However, despite the many theories proposed to explain the tropical interannual variability of ENSO [*Jin*, 1997; *Neelin et al*., 1998, and others], few observationally constrained theories exist to explain the sources of tropical decadal variance itself [*Dommenget and Latif*, 2008; *Clement et al*., 2011]. We hypothesize that the observed ENSO-like pattern of decadal variability arises from the combined action of ENSO and the Pacific meridional mode [*Chiang and Vimont*, 2004].

2. Hypothesis for Pacific Climate Variability

On interannual timescales the ENSO system dominates the tropical variance. Perturbations in the tropical Pacific sea surface temperature and thermocline associated with stochastic atmospheric forcing (e.g., westerly

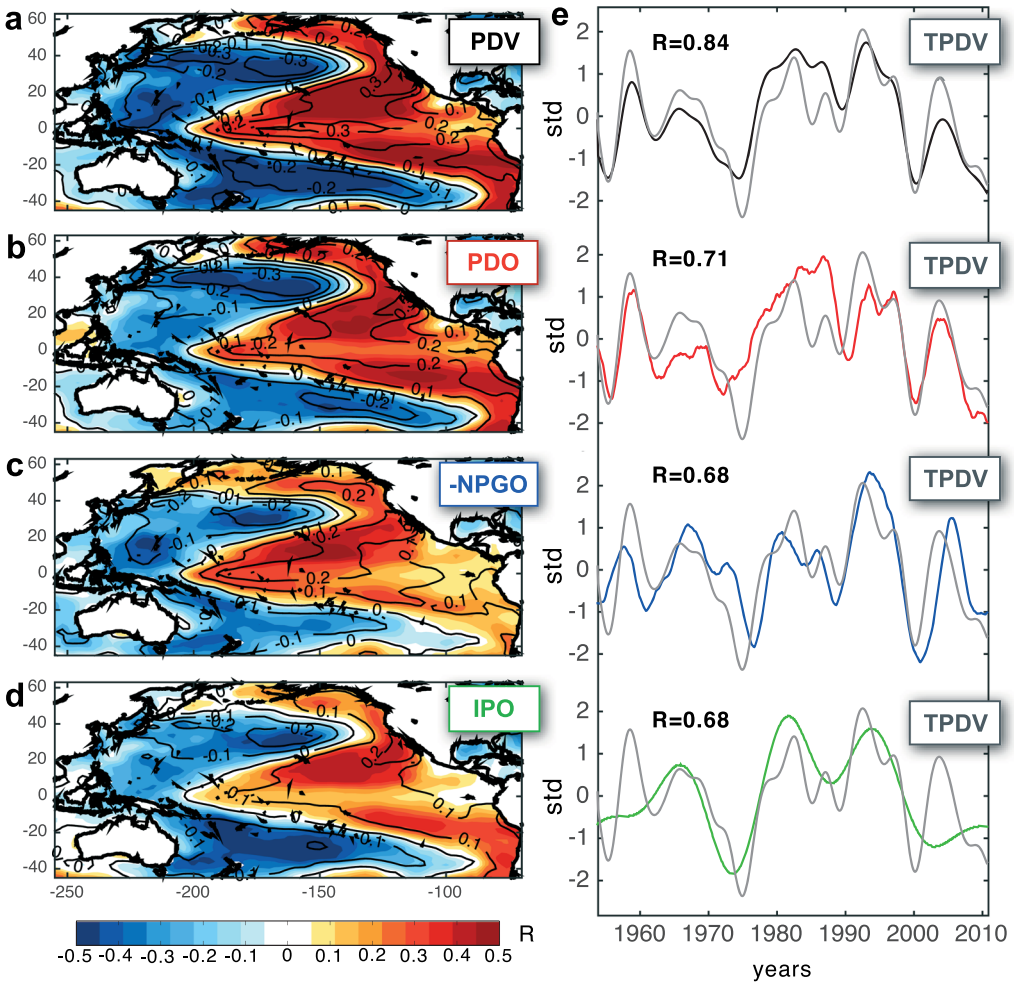

Figure 1. ENSO-like pattern of Pacific low-frequency variability. Correlation maps between monthly NOAA ERSST.v3 SSTa and (a) Pacific decadal variability (PDV) index defined as the PC1 of 8 year low-pass SSTa over Pacific basin (45°S–65°N), (b) 8 year low-pass Pacific Decadal Oscillation (PDO) index, (c) 8 year low-pass negative North Pacific Gyre Oscillation (NPGO) index, and (d) Interdecadal Pacific Oscillation (IPO) index. Regression coefficients are shown as black contours in units of °C. The time series of the indices are shown in Figure 1e and compared against a Tropical Pacific Decadal Variability (TPDV) index defined as PC1 of 8 year low-pass SST over the equatorial Pacific (12°S–12°N).

wind bursts) can be amplified by positive feedbacks (e.g., zonal current and thermocline feedback) that involve coupling between the atmosphere and ocean dynamics [*Bjerknes*, 1969; *Suarez and Schopf*, 1988; *Jin*, 1997]. These positive feedbacks allow for the growth of dynamical modes along the equatorial zonal plane (e.g., zonal modes) that are collectively referred to as ENSO.

Although the dynamics of zonal modes are important in supporting and driving the ENSO system at the equator, several studies show that extratropical stochastic atmospheric forcing can also energize ENSO variance through thermodynamic and dynamic feedbacks [*Vimont et al.*, 2003; *Chiang and Vimont*, 2004; *Anderson and Perez*, 2015]. Most importantly, for this study, it has been shown that the high-frequency variability of the North Pacific Oscillation (NPO) [*Rogers*, 1981; *Linkin and Nigam*, 2008] can generate winds and SSTa in the subtropics that amplify and propagate into the tropical Pacific through the wind-evaporation-SST (WES) feedback [*Xie*, 1999]. These sets of dynamical modes operate primarily along the north-south meridional plane and are referred to as meridional modes (MM). The imprint of meridional mode dynamics is evident in the SSTa and sea level pressure anomalies (SLPa) patterns of the ENSO extratropical precursors with a lead of 6–12 months, both for eastern and central Pacific El Niño events (Figure 2) [see also *Penland and Sardeshmukh*, 1995; *Vimont et al.*, 2003; *Anderson*, 2003; *Zhang et al.*, 2014]. These and other findings

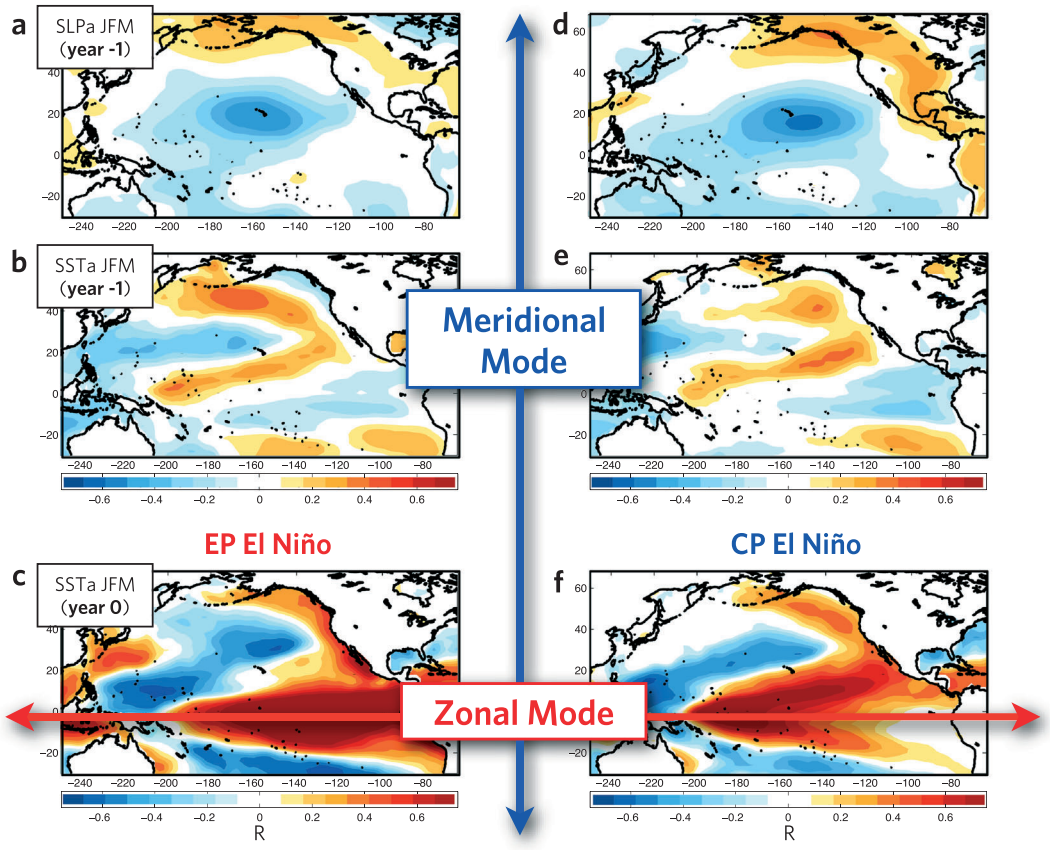

Figure 2. Precursor patterns to ENSO. Correlation map between winter (January–March (JFM)) Niño34 index and (a) SLPa in the prior winter, (b) SSTa in the prior winter, and (c) with concurrent SSTa. (e–g) The same analysis done with the CPW index is shown.

[*Chiang and Vimont*, 2004; *Chang et al*., 2007; *Alexander et al*., 2010] show that extratropical stochastic forcing (e.g., NPO) energize the interannual variance in the tropical Pacific through meridional mode dynamics (although not exclusively [*Anderson et al*., 2013]). Given that the dynamics of the meridional mode are consistent with a red noise process without any preferential timescales [*Larson and Kirtman*, 2013], it is plausible that meridional modes also play an important role in energizing the decadal and multidecadal energy of the tropical Pacific. As initial support for this hypothesis, we note that in the Atlantic basin where ENSO feedbacks are very weak, the dominant mode of tropical variability is controlled by meridional mode dynamics and is characterized by energy on the decadal and longer timescales [*Chiang and Vimont*, 2004; *Xie and Carton*, 2013].

Building on these previous findings, we develop a red noise null hypothesis for Pacific decadal and multidecadal variability (Figure 3) whereby the NPO stochastic forcing in the extratropics excites meridional modes in the subtropics, which inject decadal-scale variance into the tropical system through the propagation of SSTa along the north-south plane (Figure 3, step 1). In the tropics, these SSTa are amplified by zonal mode dynamics (e.g., ENSO) and excite teleconnections that project the decadal-scale variance back into the extratropics (Figure 3, step 2). The extratropical projection of the decadal variance impacts both PDO and NPGO depending on the interannual state of ENSO. For example, while eastern Pacific ENSO teleconnections preferentially energize the PDO pattern [e.g., *Alexander et al*., 2002; *Newman et al*., 2003; *Deser et al*., 2004], central Pacific ENSO events project onto the NPGO [e.g., *Di Lorenzo et al*., 2010; *Furtado et al*., 2012]. This hypothesis, which we will refer to as the *Pacific climate null hypothesis*, is essentially a red noise process [*Frankignoul and Hasselmann*, 1977], where the forcing is given by the atmospheric stochastic variability that energizes the MM (e.g., NPO) and the damping timescale arises from spatial/temporal evolution of the coupled system response to the MM perturbation. For example, following the diagram in Figure 3, the winter time NPO-type variability in a given year energizes ENSO-like variability along the equator that peaks in the following winter

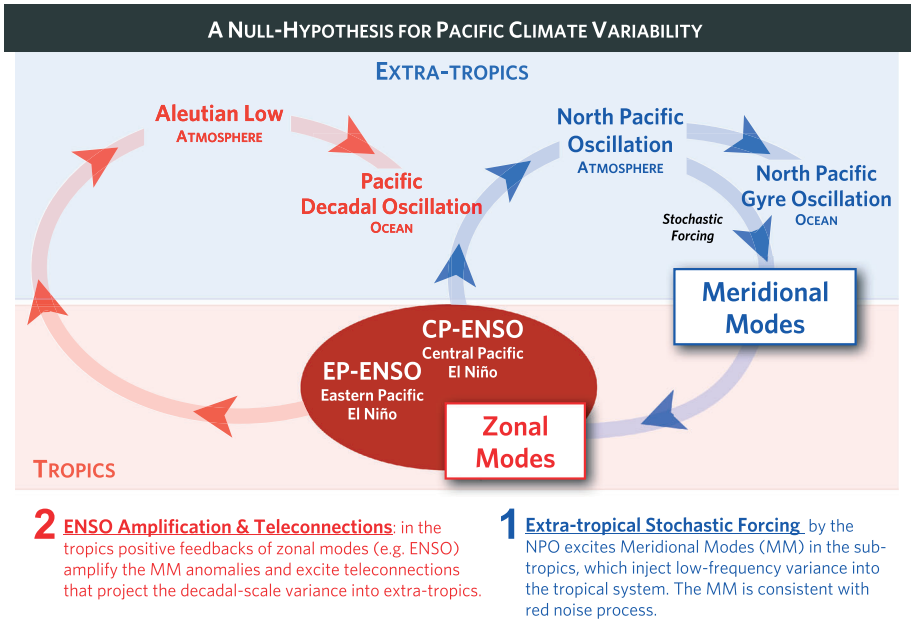

Figure 3. Diagram of the null hypothesis for Pacific climate variability. In this red noise model the stochastic variability of the North Pacific Oscillation (NPO) acts as the forcing, while the evolution of the ocean-atmosphere coupled system from extratropics to tropics and back to extratropics (1–2 years) provides the damping timescale. This progression and timescale provide the key memory for integrating the stochastic forcing of the atmosphere (e.g., NPO) into decadal-scale variance over the entire Pacific basin, beyond the generation region of the MM (see text for a detailed discussion).

(~12 months) [*Anderson*, 2003; *Vimont et al.*, 2003]. In turn, the ENSO teleconnections drive changes in the extratropical atmosphere, which drive ocean anomalies in the extratropics (e.g., SSTa) that decay over a period of 6–12 months [*Schneider and Cornuelle*, 2005]. The timescale resulting from this progression is ~18–24 months, which we interpret as the characteristic damping timescale in the red noise model. If we also account for the existence of feedbacks between ENSO and the MM (e.g., Central Pacific ENSO projecting onto NPO) [*Di Lorenzo et al.*, 2010; *Furtado et al.*, 2012], the low-frequency variance is further enhanced because the NPO spectrum is redden (e.g., driving an autoregressive model of order 1 with red noise provides a strong low-frequency filter).

The Pacific climate null hypothesis is consistent with previous theories and modeling work on stochastic Pacific climate variability [*Newman et al.*, 2011] and global-scale Hyper Modes [*Dommenget and Latif*, 2008], which highlight the important interaction between the stochastic development of SSTa in the tropics (e.g., red noise process) and tropical atmospheric teleconnections in generating global multidecadal SSTa.

3. Observations and Models

Observations used for testing the Pacific climate null hypothesis (Figure 3) originate from two keys sources. SST data and anomalies are derived from the National Oceanic and Atmospheric Administration (NOAA) Extended Reconstruction SST, version 3 (ERSST.v3) product [*Smith and Reynolds*, 2004]. Monthly mean fields are available on a 2° × 2° horizontal grid globally, with data available from 1854 to the present. For our work, we restrict the period of record to 1950–2012 to match the other data sets. Monthly mean SLP data and anomalies are taken from the National Centers for Environmental Prediction-National Center for Atmospheric Research reanalysis product [*Kalnay et al.*, 1996] and exist on a 2.5° × 2.5° horizontal grid globally. For both observational products, we restrict our analysis primarily to the Pacific basin (i.e., 100°E–60°W, 45°S–65°N).

To diagnose the role of meridional modes, two sets of coupled ocean-atmosphere modeling experiments are conducted using the International Center for Theoretical Physics (ICTP) atmosphere general circulation model (AGCM) coupled to a 100 m slab ocean. This AGCM, also known as SPEEDY, uses eight vertical layers and T30 horizontal resolution (3.758 3 3.758 on a longitude-latitude grid). Climatological heat fluxes corrected through

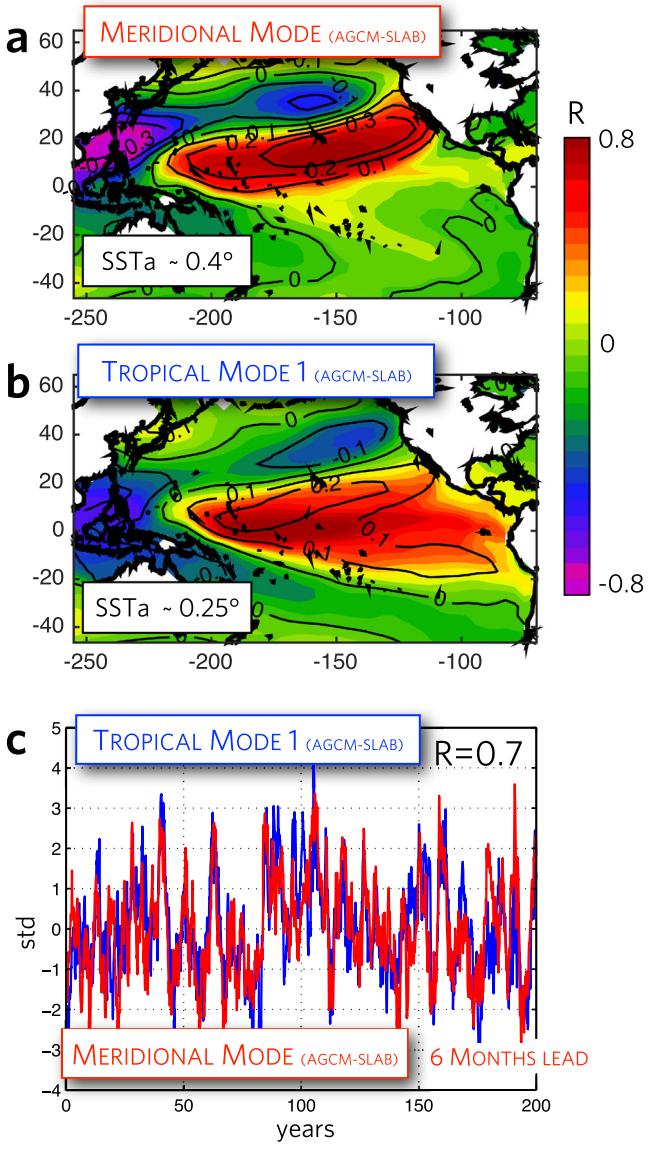

Figure 4. Tropical decadal variability of the meridional model experiment. (a) Correlation maps between monthly 2000 year long model SSTa and North Pacific meridional mode monthly index defined as PC1 of subtropical SSTa between (12°N–30°N). (b) Correlation maps between monthly model SSTa and monthly PC1 of tropical SSTa between 12°S and 12°N. Regression coefficients are shown as black contours in units of °C. The size of the maximum SSTa is reported in the bottom left of the panels. (c) Six month lead correlation between model meridional mode index (red line) and tropical PC1 (blue line) (shown only for the first 200 years).

observations are prescribed to account for ocean heat transport. The physical parameterizations of the model are described in *Molteni* [2003], and prior applications of this configuration can be found in *Bracco et al.* [2004]. The experimental designs are as follows.

3.1. The Zonal Mode Experiment

This experiment isolates the fraction of Pacific decadal variance that is deterministically forced within the equatorial Pacific and filters out any stochastic contributions from the MM. SSTa from 1950 to 2012 are prescribed in a narrow region in the equatorial Pacific (12°S–12°N) as a surface boundary condition to drive a 45-member ensemble of the ICTP AGCM with the slab ocean. Away from this tropical region, interactive fluxes between the AGCM and the slab ocean are implemented to determine the SSTa field. By examining the ensemble mean SSTa from the 45 members, we effectively remove all contributions of stochastic forcing from the extratropics and therefore identify the SSTa variance that is driven by the equatorial Pacific.

3.2. The Meridional Mode Experiment

This experiment removes zonal mode dynamics and only retains thermodynamic coupling representative of MM dynamics. For this experiment, we perform a 2000 year integration of the AGCM with the interactive slab ocean over the entire global ocean. The absence of a dynamical ocean in the AGCM slab ocean model effectively removes the positive feedbacks of zonal modes (e.g., ENSO) along the equatorial plane while preserving the MM dynamics that rely on thermodynamic coupling (e.g., the WES feedback). To verify that tropical decadal variability in this experiment is driven by MMs we analyze the relationship between the dominant modes of SSTa variability in the subtropical North Pacific (12°N–30°N) and the tropical Pacific (12°S–12°N). In the subtropics, the leading empirical orthogonal function (EOF) of monthly SSTa exhibits the characteristic pattern of MMs (Figure 4a), while the leading EOF of monthly SSTa in the tropics exhibits maximum loading in the central tropical Pacific (i.e., around 180°W) consistent with the observed pattern of SSTa decadal variance (Figure 4b). The principal component (PC) time series of the modes exhibit strong low-frequency variability (Figure 4c), which is consistent with a red noise spectrum. The cross correlation between the leading subtropical and tropical PCs reaches a maximum correlation

of $R = 0.7$ when the subtropical PC leads the tropical PC by 6 months (Figure 4c). This 6 month lead timescale agrees with the characteristic timescale of growth and propagation of the North Pacific MM into the equatorial Pacific [e.g., *Penland and Sardeshmukh*, 1995; *Vimont et al*., 2003; *Vimont*, 2010; *Alexander et al*., 2008].

This analysis confirms that the largest fraction of tropical low-frequency variability in this experiment is the results of meridional mode dynamics and that the MM can generate significant decadal variance. For this reason, we refer to this run as the MM experiment, although the MM is not the only active dynamics.

4. Testing the Pacific Decadal Null Hypothesis

To test the tropical Pacific climate null hypothesis, we first characterize the observed spatial and temporal evolution of the tropical decadal variance associated with ENSO-like decadal pattern (Figure 1). After applying an 8 year low-pass filter to the observed SSTa, we perform a principal component analysis in the tropical Pacific (12°S–12°N) to extract the decadal-scale variability in the tropics. The first EOF explains about 50% of the total low-frequency variance, and its eigenvalue is well separated from subsequent eigenvalues. A correlation of the leading PC time series (PC1) with the monthly SSTa over the entire Pacific basin reveals the characteristic pattern of ENSO-like decadal variability in the Pacific (Figure 5b, compare with Figure 1). Furthermore, PC1 is correlated with the low-frequency component (8 year low pass) of other indices of Pacific decadal variability including the Interdecadal Pacific Oscillation (IPO) ($R = 0.68$), the PDO ($R = 0.71$), and the NPGO ($R = 0.68$) and shares a similar spatial structure especially in the tropics where all these modes significantly overlap (Figure 1). To characterize the growth and decay of this ENSO-like pattern, we compute 1.5 year lead and lag correlation maps of PC1 with Pacific monthly SSTa (Figures 5a and 5c). The 1.5 year timescale is chosen as it is the approximate *e*-folding timescale of the PC1 autocorrelation function (~1.67 years). Inspecting the lead and lag correlation maps (Figures 5a and 5c) reveals that the spatial patterns of the growing and decaying phases are not identical, indicating that the spatial expression of the autocorrelation function is not symmetric in space. The growing phase pattern (i.e., Figure 5a) exhibits a stronger loading pattern in the North Pacific resembling the pattern associated with the Pacific MM (compare Figure 5a with Figures 2c and 2e). By contrast, the decaying phase (Figure 5c) exhibits a more equatorially symmetric SSTa correlation pattern representative of the well-known ENSO teleconnection patterns.

Using the model experiments, our goal is to show that the meridional mode dynamics controls the growing phase of the ENSO-like decadal pattern, while zonal mode dynamics (e.g., ENSO) controls the decaying phase pattern. To do so, we examine the zonal mode and meridional mode AGCM experiments, which selectively exclude/include the contributions of the meridional mode dynamics.

We first examine the evolution of the ensemble mean SSTa from the zonal mode experiments which are forced with prescribed tropical SSTa forcing between 1950 and 2012. By construction, the ensemble mean SSTa removes all the variance contributions associated with extratropical stochastic forcing and meridional modes, and in the tropical forcing region (12°S–12°N) the evolution of the SSTa is identical to the observed. We compute the lead/lag correlation maps between the observed low-frequency PC1 of SSTa and the model monthly SSTa. We find that at lag 0 years (Figure 5e) and at lag 1.5 year (the decaying phase, Figure 5f) the model reproduces the observed structure of the ENSO-like decadal variability in the extratropics with anomaly correlation patterns (ACPs) ranging between ACP = 0.6 and 0.8, in the decaying and peak phase, respectively. However, at lead 1.5 year (Figure 5d) the model is unable to capture the North Pacific growing structure of the decadal pattern ($ACP_{NP} = 0$). This absence suggests that tropical forcing (e.g., ENSO) alone cannot explain the growing phase of the ENSO-like decadal variability. Although the North Pacific signal is missing in the growing phase, in the South Pacific we find a signature of the ENSO-like decadal variability ($ACP_{SP} = 0.62$), implying that a fraction of the precursor pattern in the South Pacific is forced by tropical dynamics (Figure 5d).

We now examine the meridional mode experiment using the 2000 year long integration of the AGCM slab coupled model. We have already verified that the dominant fraction of tropical variability in this model is contributed by the North Pacific meridional mode (e.g., Figure 4). An examination of the growing and decaying phases of the decadal pattern associated with the model tropical low-pass SSTa PC1 reveals that the inclusion of meridional mode dynamics allows us to recover the growing phase of the ENSO-like decadal pattern (Figure 5g; $ACP_{NP} = 0.68$). However, the decaying phase (Figure 5e) does not resemble the observations ($ACP_{NP} = 0$) and most of the decay occurs along the equatorial Pacific with little signs of robust symmetric

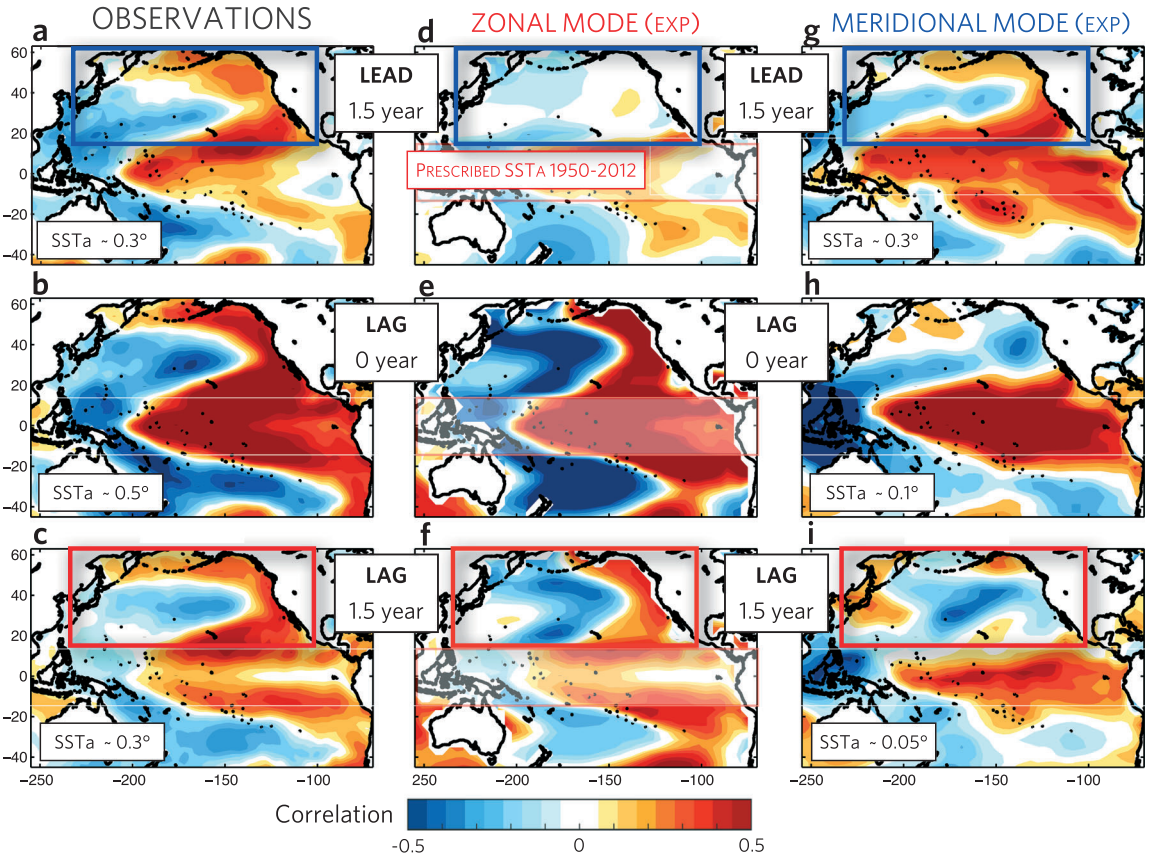

Figure 5. Spatial structure and temporal evolution of ENSO-like pattern of decadal variance in observations and models. Correlation between the observed tropical PC1 of 8 year low-pass SSTa defined between 12°S and 12°N and monthly mean SSTa at (a) lead 1.5 year the growing phase, (b) lag 0 the peak, and (c) lag 1.5 year the decaying phase. Same analysis done for the zonal mode experiments (d) growing, (e) peak, and (f) decaying phases. The white shadowing in Figures 5d–5f denotes the region where prescribed SSTa forcing was used in the zonal mode experiments. Same analysis done for the meridional mode experiment (g) growing, (h) peak, and (i) decaying phases. The average size of the SSTa in the regions of maximum correlation loading is indicated for the observations and meridional mode experiments in bottom left corner of each panel.

teleconnections from the tropics into the extratropics, which are visible in the observations. To understand the nature of this local decay in the tropics, we compute the average size of the SSTa in the high loading regions of the growing and decaying phases. In the growing phase we find that both observations and the meridional mode experiment have an amplitude of ~0.3 C (compare Figure 5a with Figure 5g). However, at lag 0, while the SSTa of observations in the tropics continues to grow reaching ~0.5 C, in the meridional mode experiment the lack of zonal mode feedbacks (e.g., ENSO) prevents this anomaly from growing and instead negative feedbacks (e.g., damping) reduce the SSTa to ~0.1 C (compare Figure 5b with Figure 5h). In the meridional mode experiment, the lack of ENSO positive feedbacks and the decay of the SSTa prevent the system from exciting ENSO teleconnections, which are important in spreading the signal back to the extratropics as seen in the observations. Therefore, in the meridional mode experiment the tropical SSTa continues to decay locally in the tropics and at lag 1.5 year (Figure 5e, the decaying phase) its amplitude is further reduced to ~0.01 C. It is interesting to note that this local decay in the tropics is not evident in the observations, which show zero anomalies. Indeed, previous studies have reported how ocean waves dynamics related to the ENSO cycle are effective in terminating the SSTa along the equator [e.g., *Neelin et al.*, 1998].

Before concluding, we also note that the growing phase of the MM experiment exhibits correlations along the entire equatorial strip, while observations show correlation only in the central tropical Pacific region. This difference is related to the dominant low-frequency character of the MM and tropical variability in the MM experiment (see time series Figure 4c). This implies that correlations computed with the low-pass PC1 of SSTa capture this low-frequency signal. This is not true using the monthly data where we find no correlation in the tropics at lead 6 months (Figure 4). In the observations, ENSO interannual dynamics and

the cold tongue upwelling region variability act as source for noise in the eastern tropical Pacific reducing the signal-to-noise ratio between the low-frequency expression of the MM in the extratropics at lead 1.5 years and the tropics at lag 0 year. Also, in the peak phase of the MM experiment, the amplitude of the SSTa in the tropics is smaller (~0.1 C) than at lead 1.5 year (~0.3 C), confirming that the dominant tropical mode is the manifestation of the decay of the Pacific meridional mode, which has originated in the subtropics earlier (see Figure 4, regression contours).

5. Summary and Discussion

Through analyses of the decadal variance of Pacific-wide SSTa in both observations and coupled ocean-atmosphere simulations, we offer significant evidence that the ENSO-like pattern of Pacific decadal variability arises from the interaction of meridional modes (e.g., MM) and the zonal modes (e.g., ENSO). While more sophisticated coupled model experiments are needed to separate the fraction of decadal variability that is driven by ENSO versus MMs, the main conclusion of our work is that the structure and evolution of the ENSO-like Pacific decadal variability (e.g., the growing and decaying phases) cannot be explained by the zonal mode (e.g., ENSO) or the MM in isolation. Although both modes can generate low-frequency variance in isolation, the interaction between both modes is required to explain the observations. In the growing phase, the MM supplies an important source of low-frequency variance through integration of extratropical stochastic atmospheric forcing (e.g., red spectrum), while the zonal mode dynamics (i.e., ENSO) amplify and distribute that low-frequency energy in the peak and decaying phases through global teleconnections. We refer to this mechanism as the Pacific climate null hypothesis (as summarized in Figure 3) because the temporal dynamics energizing this evolution are consistent with a red noise process. However, the spatial progression of this ENSO-like decadal variance relies on specific patterns associated with the tropical coupled ocean/atmosphere response to the atmospheric stochastic forcing (e.g., MM and ENSO), and its teleconnected imprints in the extratropics (e.g., PDO, NPGO, and IPO). This red noise hypothesis is consistent with previous studies exploring Pacific decadal variance in a hierarchy of models, from linear inverse models [*Newman et al*., 2011] to AGCMs coupled to ocean mixed layers [*Dommenget and Latif*, 2008; *Clement et al*., 2011] and fully coupled climate models [*Yeh and Kirtman*, 2004].

Interestingly, the growth rates associated with the thermodynamic feedback of the MMs depend on the mean SST in subtropical and tropical regions [*Vimont*, 2010]. Hence, anticipated warming of global surface SSTs may amplify the SSTa associated with the growth of the MM. Using our new framework as a guide, this amplification would energize both the interannual and decadal variance of the entire Pacific basin (Figure 3). Consistent with this hypothesis, recent studies have suggested that the link between the North Pacific ENSO precursor pattern (e.g., NPO) and ENSO increases under enhanced greenhouse warming [e.g., *Wang et al*., 2013, 2014]. Actual quantification of this amplification and of the effects on ENSO and MM are aims for future studies.

These results provide an alternative set of dynamics that initiate and energize the Pacific decadal variability independently of ENSO and of other subsurface or wave dynamics [e.g., *Pierce et al*., 2000; *Solomon et al*., 2008]. The mechanism and forcing controlling these dynamics and their interaction with the ENSO system may prove useful as a framework for examining climate change projections for Pacific decadal variability in climate models, which may not reproduce the correct spatial patterns of the observed decadal dynamics, yet may capture the underlying dynamics of interaction between zonal and meridional modes, along with the atmospheric forcing patterns that energize their variance.

Acknowledgments
We acknowledge the support of the NSF-OCE 1356924, NSF-OCE 1419292, NSF OCE-0550266, NSF 1357015, DOE-DESC000511 and JAMSTEC-IPRC Joint Investigations. The modeling data used in this study are available at www.podx.org.

References

Alexander, M. A., I. Blade, M. Newman, J. R. Lanzante, N. C. Lau, and J. D. Scott (2002), The atmospheric bridge: The influence of ENSO teleconnections on air-sea interaction over the global oceans, *J. Clim.*, *15*(16), 2205–2231, doi:10.1175/1520-0442(2002)015<2205:tabtio>2.0.co;2.

Alexander, M. A., L. Matrosova, C. Penland, J. D. Scott, and P. Chang (2008), Forecasting Pacific SSTs: Linear inverse model predictions of the PDO, *J. Clim.*, *21*(2), 385–402, doi:10.1175/2007jcli1849.1.

Alexander, M. A., D. J. Vimont, P. Chang, and J. D. Scott (2010), The impact of extratropical atmospheric variability on ENSO: Testing the seasonal footprinting mechanism using coupled model experiments, *J. Clim.*, *23*(11), 2885–2901, doi:10.1175/2010jcli3205.1.

Anderson, B., and R. Perez (2015), ENSO and non-ENSO induced charging and discharging of the equatorial Pacific, *Clim. Dyn.*, 1–19, doi:10.1007/s00382-015-2472-x.

Anderson, B. T. (2003), Tropical Pacific sea-surface temperatures and preceding sea level pressure anomalies in the subtropical North Pacific, *J. Geophys. Res.*, *108*(D23), 4732, doi:10.1029/2003JD003805.

Anderson, B. T., R. C. Perez, and A. Karspeck (2013), Triggering of El Niño onset through trade wind-induced charging of the equatorial Pacific, *Geophy. Res. Lett.*, *40*, 1212–1216, doi:10.1002/grl.50200.

Bjerknes, J. (1969), Atmospheric teleconnections from equatorial Pacific, *Mon. Weather Rev.*, *97*(3), 163–172, doi:10.1175/1520-0493(1969)097<0163:Atftep>2.3.Co;2.
Bracco, A., F. Kucharski, R. Kallummal, and F. Molteni (2004), Internal variability, external forcing and climate trends in multi-decadal AGCM ensembles, *Clim. Dyn.*, *23*(6), 659–678, doi:10.1007/S00382-004-0465-2.
Chang, P., L. Zhang, R. Saravanan, D. J. Vimont, J. C. H. Chiang, L. Ji, H. Seidel, and M. K. Tippett (2007), Pacific meridional mode and El Nino–Southern Oscillation, *Geophys. Res. Lett.*, *34*, L16608, doi:10.1029/2007GL030302.
Chiang, J. C. H., and D. J. Vimont (2004), Analogous Pacific and Atlantic meridional modes of tropical atmosphere–ocean variability, *J. Clim.*, *17*(21), 4143–4158, doi:10.1175/Jcli4953.1.
Clement, A., P. DiNezio, and C. Deser (2011), Rethinking the ocean's role in the Southern Oscillation, *J. Clim.*, *24*(15), 4056–4072, doi:10.1175/2011jcli3973.1.
Deser, C., A. S. Phillips, and J. W. Hurrell (2004), Pacific interdecadal climate variability: Linkages between the tropics and the North Pacific during boreal winter since 1900, *J. Clim.*, *17*(16), 3109–3124, doi:10.1175/1520-0442(2004)017<3109:Picvlb>2.0.Co;2.
Di Lorenzo, E., et al. (2008), North Pacific Gyre Oscillation links ocean climate and ecosystem change, *Geophys. Res. Lett.*, *35*, L08607, doi:10.1029/2007GL032838.
Di Lorenzo, E., K. M. Cobb, J. C. Furtado, N. Schneider, B. T. Anderson, A. Bracco, M. A. Alexander, and D. J. Vimont (2010), Central Pacific El Niño and decadal climate change in the North Pacific Ocean, *Nat. Geosci.*, *3*(11), 762–765, doi:10.1038/Ngeo984.
Dommenget, D., and M. Latif (2008), Generation of hyper climate modes, *Geophys. Res. Lett.*, *35*, L02706, doi:10.1029/2007GL031087.
Frankignoul, C., and K. Hasselmann (1977), Stochastic climate models. Part II: Application to sea surface temperature anomalies and thermocline variability, *Tellus*, *29*, 289–305.
Furtado, J. C., E. Di Lorenzo, B. T. Anderson, and N. Schneider (2012), Linkages between the North Pacific Oscillation and central tropical Pacific SSTs at low frequencies, *Clim. Dyn.*, *39*(12), 2833–2846, doi:10.1007/s00382-011-1245-4.
Jin, F. F. (1997), An equatorial ocean recharge paradigm for ENSO. 1. Conceptual model, *J. Atmos. Sci.*, *54*(7), 811–829, doi:10.1175/1520-0469(1997)054<0811:Aeorpf>2.0.Co;2.
Kalnay, E., et al. (1996), The NCEP/NCAR 40-Year Reanalysis Project, *Bull. Am. Meteorol. Soc.*, *77*(3), 437–471, doi:10.1175/1520-0477(1996)077<0437:tnyrp>2.0.co;2.
Larson, S., and B. Kirtman (2013), The Pacific meridional mode as a trigger for ENSO in a high-resolution coupled model, *Geophys. Res. Lett.*, *40*, 3189–3194, doi:10.1002/grl.50571.
Linkin, M. E., and S. Nigam (2008), The North Pacific Oscillation–West Pacific teleconnection pattern: Mature-phase structure and winter impacts, *J. Clim.*, *21*(9), 1979–1997, doi:10.1175/2007jcli2048.1.
Mantua, N. J., S. R. Hare, Y. Zhang, J. M. Wallace, and R. C. Francis (1997), A Pacific interdecadal climate oscillation with impacts on salmon production, *Bull. Am. Meteorol. Soc.*, *78*(6), 1069–1079, doi:10.1175/1520-0477(1997)078<1069:Apicow>2.0.Co;2.
Molteni, F. (2003), Atmospheric simulations using a GCM with simplified physical parameterization. I: Model climatology and variability in multi-decadal experiments, *Clim. Dyn.*, *20*, 175–191.
Neelin, J. D., D. S. Battisti, A. C. Hirst, F. F. Jin, Y. Wakata, T. Yamagata, and S. E. Zebiak (1998), ENSO theory, *J. Geophys. Res.*, *103*(C7), 14,261–14,290, doi:10.1029/97JC03424.
Newman, M., G. P. Compo, and M. A. Alexander (2003), ENSO-forced variability of the Pacific Decadal Oscillation, *J. Clim.*, *16*(23), 3853–3857, doi:10.1175/1520-0442(2003)016<3853:Evotpd>2.0.Co;2.
Newman, M., M. Alexander, and J. D. Scott (2011), An empirical model of tropical ocean dynamics, *Clim. Dyn.*, *37*, 1823–1841, doi:10.1007/s00382-011-1034-0.
Penland, C., and P. D. Sardeshmukh (1995), The optimal-growth of tropical sea-surface temperature anomalies, *J. Clim.*, *8*(8), 1999–2024, doi:10.1175/1520-0442(1995)008<1999:Togots>2.0.Co;2.
Pierce, D. W., T. P. Barnett, and M. Latif (2000), Connections between the Pacific Ocean tropics and midlatitudes on decadal timescales, *J. Clim.*, *13*(6), 1173–1194, doi:10.1175/1520-0442(2000)013<1173:Cbtpot>2.0.Co;2.
Power, S., T. Casey, C. Folland, A. Colman, and V. Mehta (1999), Inter-decadal modulation of the impact of ENSO on Australia, *Clim. Dyn.*, *15*(5), 319–324, doi:10.1007/S003820050284.
Rogers, J. C. (1981), The North Pacific Oscillation, *Int. J. Climatol.*, *1*(1), 39–57, doi:10.1002/joc.3370010106.
Schneider, N., and B. D. Cornuelle (2005), The forcing of the Pacific Decadal Oscillation, *J. Clim.*, *18*(21), 4355–4373, doi:10.1175/jcli3527.1.
Smith, T. M., and R. W. Reynolds (2004), Improved extended reconstruction of SST (1854–1997), *J. Clim.*, *17*(12), 2466–2477, doi:10.1175/1520-0442(2004)017<2466:Ieros>2.0.Co;2.
Solomon, A., S.-I. Shin, M. Alexander, and J. McCreary (2008), The relative importance of tropical variability forced from the North Pacific through ocean pathways, *Clim. Dyn.*, *31*(2–3), 315–331, doi:10.1007/s00382-007-0353-7.
Suarez, M. J., and P. S. Schopf (1988), A delayed action oscillator for ENSO, *J. Atmos. Sci.*, *45*(21), 3283–3287, doi:10.1175/1520-0469(1988)045<3283:Adaofe>2.0.Co;2.
Trenberth, K. E., and J. W. Hurrell (1994), Decadal atmosphere–ocean variations in the Pacific, *Clim. Dyn.*, *9*(6), 303–319, doi:10.1007/bf00204745.
Vimont, D. J. (2005), The contribution of the interannual ENSO cycle to the spatial pattern of decadal ENSO-like variability, *J. Clim.*, *18*(12), 2080–2092, doi:10.1175/Jcli3365.1.
Vimont, D. J. (2010), Transient growth of thermodynamically coupled variations in the tropics under an equatorially symmetric mean, *J. Clim.*, *23*(21), 5771–5789, doi:10.1175/2010jcli3532.1.
Vimont, D. J., J. M. Wallace, and D. S. Battisti (2003), The seasonal footprinting mechanism in the Pacific: Implications for ENSO, *J. Clim.*, *16*(16), 2668–2675, doi:10.1175/1520-0442(2003)016<2668:Tsfmit>2.0.Co;2.
Wang, S. Y., M. L'Heureux, and J. H. Yoon (2013), Are greenhouse gases changing ENSO precursors in the Western North Pacific?, *J. Clim.*, *26*(17), 6309–6322, doi:10.1175/jcli-d-12-00360.1.
Wang, S. Y., L. Hipps, R. R. Gillies, and J. H. Yoon (2014), Probable causes of the abnormal ridge accompanying the 2013–2014 California drought: ENSO precursor and anthropogenic warming footprint, *Geophys. Res. Lett.*, *41*, 3220–3226, doi:10.1002/2014GL059748.
Xie, S. P. (1999), A dynamic ocean–atmosphere model of the tropical Atlantic decadal variability, *J. Clim.*, *12*(1), 64–70, doi:10.1175/1520-0442-12.1.64.
Xie, S.-P., and J. A. Carton (2013), Tropical Atlantic variability: Patterns, mechanisms, and impacts, in *Earth's Climate*, edited by C. Wang, S. P. Xie and J. A. Carton, pp. 121–142, AGU, Washington, D. C., doi:10.1029/147gm07.
Yeh, S.-W., and B. P. Kirtman (2004), Tropical Pacific decadal variability and ENSO amplitude modulation in a CGCM, *J. Geophys. Res.*, *109*, C11009, doi:10.1029/2004JC002442.
Zhang, Y., J. M. Wallace, and D. S. Battisti (1997), ENSO-like interdecadal variability: 1900–93, *J. Clim.*, *10*(5), 1004–1020, doi:10.1175/1520-0442(1997)010<1004:eliv>2.0.co;2.
Zhang, H., et al. (2014), The South Pacific meridional mode: A mechanism for ENSO-like variability, *J. Clim.*, *27*(2), 769–783.